Gas-Phase Preparation of the 14π Hückel Polycyclic Aromatic Anthracene and Phenanthrene Isomers (C$_{14}$H$_{10}$) via the Propargyl Addition–BenzAnnulation (PABA) Mechanism

Chang Yang Wang,[a] Long Zhao,*[b] and Ralf I. Kaiser*[c]

Polycyclic aromatic hydrocarbons (PAHs) imply the missing link between resonantly stabilized free radicals and carbonaceous nanoparticles, commonly referred to as soot particles in combustion systems and interstellar grains in deep space. Whereas gas phase formation pathways to the simplest PAH – naphthalene (C$_{10}$H$_8$) – are beginning to emerge, reaction pathways leading to the synthesis of the 14π Hückel aromatic PAHs anthracene and phenanthrene (C$_{14}$H$_{10}$) are still incomplete. Here, by utilizing a chemical microreactor in conjunction with vacuum ultraviolet (VUV) photoionization (PI) of the products followed by detection of the ions in a reflectron time-of-flight mass spectrometer (ReTOF-MS), the reaction between the 1′- and 2′-methylnaphthyl radicals (C$_{11}$H$_9$•) with the propargyl radical (C$_3$H$_3$•) accesses anthracene (C$_{14}$H$_{10}$) and phenanthrene (C$_{14}$H$_{10}$) via the Propargyl Addition–BenzAnnulation (PABA) mechanism in conjunction with a hydrogen assisted isomerization. The preferential formation of the thermodynamically less stable anthracene isomer compared to phenanthrene suggests a kinetic, rather than a thermodynamics control of the reaction.

Introduction

Polycyclic aromatic hydrocarbons (PAHs) – organic molecules carrying fused benzene rings – with up to four rings have been recently discovered in the return samples of the Hayabusa2 spacecraft from the carbonaceous asteroid Ryugu.[1] These comprise omnipresent combustion-relevant aromatics naphthalene (C$_{10}$H$_8$), anthracene/phenanthrene (C$_{14}$H$_{10}$), fluoranthene (C$_{16}$H$_{10}$), and pyrene (C$_{16}$H$_{10}$).[2–12] Detailed ^{13}C isotopic studies[1] propose at least two distinct environments of their formation. These likely involve a traditional synthesis of aromatics in high temperature (few 1,000 K) circumstellar envelopes of carbon-rich stars along with planetary nebulae as their decedents involving the Hydrogen Abstraction – aCetylene Addition (HACA)[13–19] route together with the Phenyl Addition dehydroCyclization (PAC)[19–20] and Propargyl Addition–BenzAnnulation (PABA) mechanisms[21] as well as counterintuitive barrierless pathways like Hydrogen Abstraction Vinylacetylene Addition (HAVA),[22–29] Methylidyne Addition-Cyclization-Aromatization (MACA),[30] and Fulvenallenyl Addition Cyclization Aromatization (FACA)[31] routes operating even in cold molecular clouds at temperatures as low as 10 K.

Despite this progress, there is still a lack of a fundamental knowledge of the dominating reaction pathways leading to molecular mass growth processes of aromatics in carbon-rich circumstellar envelopes. This shortcoming is apparent considering predicted lifetimes of interstellar PAHs of some 10^8 years limited by galactic cosmic rays and shock waves,[32–35] but time scales of the injection of PAHs from circumstellar envelopes to the interstellar medium surpassing a few 10^9 years.[34] Within the framework of a bottom-up synthesis of complex aromatics from smaller PAHs, an incomplete reaction network to, e.g., two-ringed PAHs such as (substituted) naphthalenes translates not only into insufficient production rates of small PAH precursors, but also into lower formation yields of more complex aromatics. Consequently, bottom-up astrochemical networks modelling PAH synthesis must be *complete* with *all* pathways commencing from two- and three-ringed aromatics to be included (Scheme 1). The recent detection of the resonantly stabilized propargyl radical (C$_3$H$_3$•) at substantial fractional abundance relative to molecular hydrogen of 8.7×10^{-9} toward TMC-1[36] suggests that the Propargyl Addition–Benz Annulation (PABA) mechanisms[21] could play a critical role in molecular mass growth processes of aromatics in deep space.
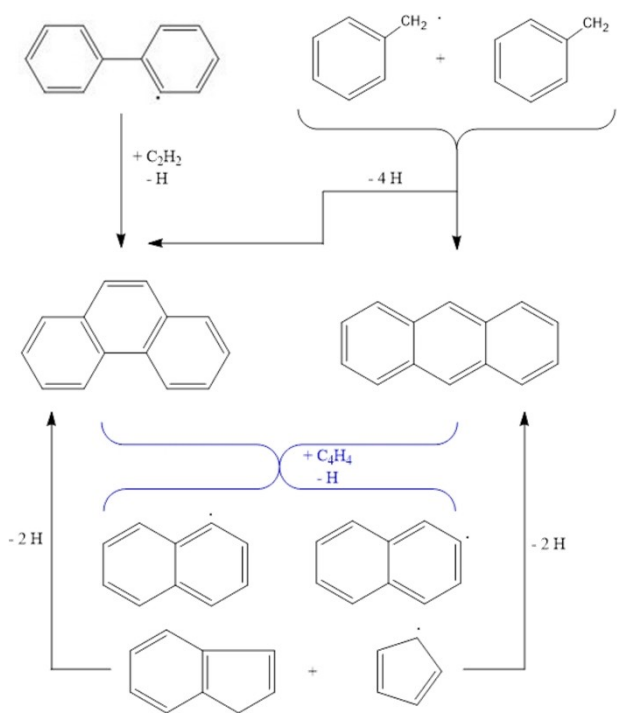
Recent chemical microreactor studies revealed that in conjunction with hydrogen assisted isomerization, the reaction of the aromatic and resonantly stabilized benzyl radical (C$_7$H$_7$•) with the propargyl radical (C$_3$H$_3$•) via PABA signifies the prototype reaction of a benzannulation of an aromatic ring carrying a benzyl moiety yielding eventually the 10π Hückel

[a] C. Y. Wang
    National Synchrotron Radiation Laboratory,
    University of Science and Technology of China,
    Hefei, Anhui 230029, China

[b] Prof. Dr. L. Zhao
    School of Nuclear Science and Technology,
    Deep Space Exploration Laboratory,
    University of Science and Technology of China
    Hefei, Anhui 230026, China
    E-mail: zhaolong@ustc.edu.cn

[c] Prof. Dr. R. I. Kaiser
    Department of Chemistry
    University of Hawaii at Manoa
    Honolulu, Hawaii, 96888, USA
    E-mail: ralfk@hawaii.edu

ChemPhysChem

Research Article
doi.org/10.1002/cphc.202400151

Chemistry Europe
European Chemical
Societies Publishing

Scheme 1. Previous molecular beams studies demonstrating the formation of anthracene and phenanthrene in the chemical microreactor. Overall barrierless pathways are color coded in blue.[21,24,40–41]

aromatic naphthalene molecule ($C_{10}H_8$).[21] In strong analogy to the benzyl–propargyl system, reactions of 1'- and 2'-methyl-naphthyl ($C_{11}H_9^\bullet$) with propargyl were predicted to eventually access anthracene ($C_{14}H_{10}$) and phenanthrene ($C_{14}H_{10}$) – a pathway which has been previously neglected in the formation of three-ringed aromatics in deep space.[21] Although 1'- and 2'-methylnaphthyl radicals ($C_{11}H_9^\bullet$) have not been detected yet in space, they likely exist as the result of photodissociation of 1- and 2-methylnaphthalene ($C_{11}H_{10}$), which in turn can be generated through the barrierless reaction of tolyl radicals ($C_6H_4CH_3$) with vinylacetylene (C_4H_4).[37–38]

Here, we reveal through an experimental study of the gas-phase reaction of 1'- and 2'-methylnaphthyl radicals ($C_{11}H_9^\bullet$) with the propargyl radical ($C_3H_3^\bullet$) in a chemical microreactor[39] in conjunction with vacuum ultraviolet (VUV) photoionization (PI) of the products followed by detection of the ions in a reflectron time-of-flight mass spectrometer (ReTOF-MS) that both anthracene ($C_{14}H_{10}$) and phenanthrene ($C_{14}H_{10}$) can be accessed via the PABA mechanism. This study affords an opportunity to provide a more 'all-inclusive' set of chemical reactions leading to the synthesis of two 14π Hückel aromatic aromatics (anthracene/phenanthrene) to be incorporated into prospective astrochemical modeling networks of carbon rich circumstellar envelopes of aging Asymptotic Giant Branch (AGB) stars.

Results and Discussion

Mass Spectra

Representative mass spectra recorded at a photon energy of 8.50 eV for the reactions of 1'-/2'-naphthylmethyl radicals ($C_{11}H_9^\bullet$) with the resonantly stabilized propargyl radical ($C_3H_3^\bullet$) are displayed in Figure 1. Control experiments were also performed by eliminating the propargyl bromide precursor (Figures. 1a and 1c). A comparison of mass spectra with and without the propargyl radical ($C_3H_3^\bullet$) provides compelling evidence on the formation of species with the molecular formulae, $C_{14}H_{10}$ (m/z = 178), $C_{14}H_{11}/^{13}CC_{13}H_{10}$ (m/z = 179), and $C_{14}H_{12}$ (m/z = 180), in the 1'- and 2'-naphthylmethyl ($C_{11}H_9^\bullet$)/ propargyl ($C_3H_3^\bullet$) systems (Figures 1b and 1d). In the reference system (Figs. 1a and 1c), ion counts at m/z = 176 and 178 are linked to the 1'- and 2'-chloromethylnaphthalene precursors ($C_{11}H_9^{35}Cl^+$ and $C_{11}H_9^{37}Cl^+$); in the blank experiments, the intensity ratios of the ion counts at m/z = 176 to 178 is about 3:1, which agrees well with the natural abundance of $^{35}Cl/^{37}Cl$. Upon the generation of propargyl radicals ($C_3H_3^\bullet$) in the reactor, the intensity of ion counts at m/z = 178 increases significantly (Figures. 1b and 1d) and eventually surpasses the ion counts of m/z = 176; further, additional signal at m/z = 180 emerged in both systems. Therefore, it can be concluded that the newly generated ion counts at m/z = 178 and 180, respectively, result from products with the molecular formulae, $C_{14}H_{10}$ (m/z = 178) and $C_{14}H_{12}$ (m/z = 180). Notably, weak signal at m/z = 179 could be linked to $C_{14}H_{11}^+$ and/or $^{13}CC_{13}H_{10}^+$. It should be noted that signals at m/z = 139 ($C_{11}H_7^+$), 140 ($C_{11}H_8^+$), 142 ($^{13}CC_{10}H_9^+/ C_{11}H_{10}^+$), and 143 ($^{13}CC_{10}H_{10}^+$) are also detectable in control experiments (Figures 1a and 1c). These species are likely
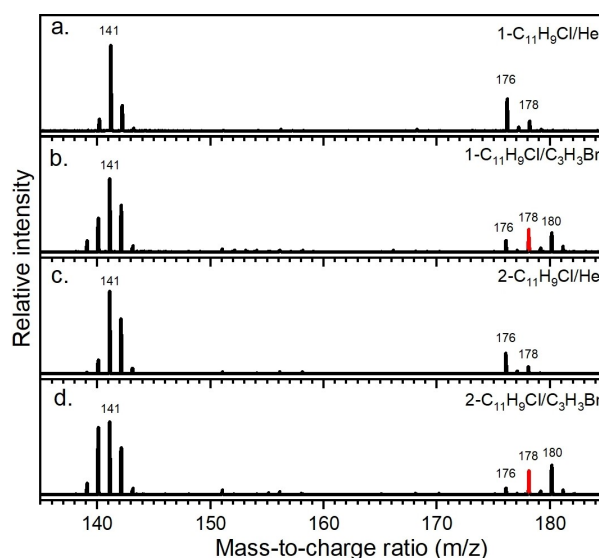

Figure 1. Representative mass spectra recorded at a photon energy of 8.50 eV at a temperature of 1,085 ± 15 K. (a) 1'-chloromethylnaphthalene ($C_{11}H_9Cl$) / helium (He) system; (b) 1'-chloromethylnaphthalene ($C_{11}H_9Cl$) / propargyl bromide (C_3H_3Br) system; (c) 2'-chloromethylnaphthalene ($C_{11}H_9Cl$) / helium (He) system; (d) 2'-chloromethylnaphthalene ($C_{11}H_9Cl$) / propargyl bromide (C_3H_3Br) system.

ChemPhysChem

Research Article
doi.org/10.1002/cphc.202400151

**Chemistry
Europe**
European Chemical
Societies Publishing

produced from the hydrogen loss and hydrogen atom addition products of the 1'-/2'-naphthylmethyl radicals (Supplementary Information Figures S2 and S3).

Photoionization Efficiency (PIE) Curves

It is our main interest not only to assign the molecular formulae of the product(s), but also to elucidate the structural isomer(s) formed. This is accomplished by a detailed inspection of the PIE curves of m/z = 178 and 179 and fitting these curves by a linear combination of known reference curves of distinct isomers of $C_{14}H_{10}$ (Figure S1). Considering the natural abundance of the ^{37}Cl isotope (32.40%), the reference curves of the precursors at m/z = 176 ($C_{11}H_9{}^{35}Cl^+$) were also recorded for the overall fit at m/z = 178 ($C_{11}H_9{}^{37}Cl^+$). For the 1'-naphthylmethyl/propargyl system (Figures 2a–2c), the onset value, 7.45 ± 0.05 eV, of the experimental PIE curve at m/z = 178 agrees well with the adiabatic ionization energy of anthracene (7.439 ± 0.006 eV[42]); however, an inclusion of a second isomer – phenathrene – is required to account for ion counts beyond 7.90 ± 0.05 eV; this value connects nicely with the adiabatic ionization energy of phenanthrene of 7.891 ± 0.001 eV.[43] Finally, a third contribution of ^{37}Cl-substituted 1-chloromethylnaphthalene was needed to provide an overall fit of the experimental PIE curve. Overall branching ratios of the ion counts for phenanthrene, anthracene, and ^{37}Cl-substituted 1-chloromethylnaphthalene were extracted to be $79.4 \pm 7.9\%$: $15.9 \pm 1.6\%$: $4.7 \pm 0.5\%$ at 8.50 eV. Accounting for the photoionization cross sections of anthracene and phenanthrene at 8.50 eV of 15.98 Mb and 9.23 Mb (PICSs),[24,44] the branching ratios of anthracene and phenanthrene are determined to be $83.5 \pm 8.4\%$ and $16.5 \pm 1.7\%$, i.e. a *dominant production of the thermodynamically less*

stable anthracene isomer. This trend is also reflected in the 2'-naphthylmethyl/propargyl system (Figures 2e–2g). Here, the experimentally recorded PIE curve at m/z = 178 could be also fit with three base functions: phenanthrene, anthracene, and the ^{37}Cl-isotopic 2-chloromethylnaphthalene with ion count ratios of $82.3 \pm 8.2\%$: $7.8 \pm 0.8\%$: $9.9 \pm 1.0\%$. Once again, accounting for the photoionization cross sections, this results in the branching ratios of anthracene and phenanthrene of $94.8 \pm 9.5\%$: $5.2 \pm 0.5\%$. For both reaction systems, it is important to highlight that ion counts at m/z = 179 ($^{13}CC_{13}H_{10}{}^+$) can be fit with the same overall branching ratios of the ion counts for ^{13}C-substituted phenanthrene, anthracene and the ^{37}Cl-isotopic 1'-/2'-chloromethylnaphthalene. To conclude, both phenanthrene and anthracene are synthesized via the reactions of two resonantly stabilized radicals – 1'-/2'-naphthylmethyl radical propargyl (reaction (1)) – with the thermodynamically less stable anthracene isomer favored. For completeness, we also provide the PIE curves at m/z = 180 for the 1'-/2'-naphthylmethyl/propargyl systems (Figures 2d and 2h). The species at m/z = 180 could be the product(s) from the reaction of 1'-naphthylmethyl ($C_{11}H_9{}^{\bullet}$, 141 amu) with propargyl ($C_3H_3{}^{\bullet}$, 39 amu) However, lacking of related reference PIE curves, it is not feasible to distinguish the structure(s). Similarly, the signal at m/z = 180 in 2'-naphthylmethyl/propargyl system could be analogous to those in 1'-naphthylmethyl/propargyl system. Note that for species at m/z = 139, 140, 141, 142 and 143, the detailed discussions are provided in Supplementary Materials with their PIE curves compiled in Figures S2–S3.
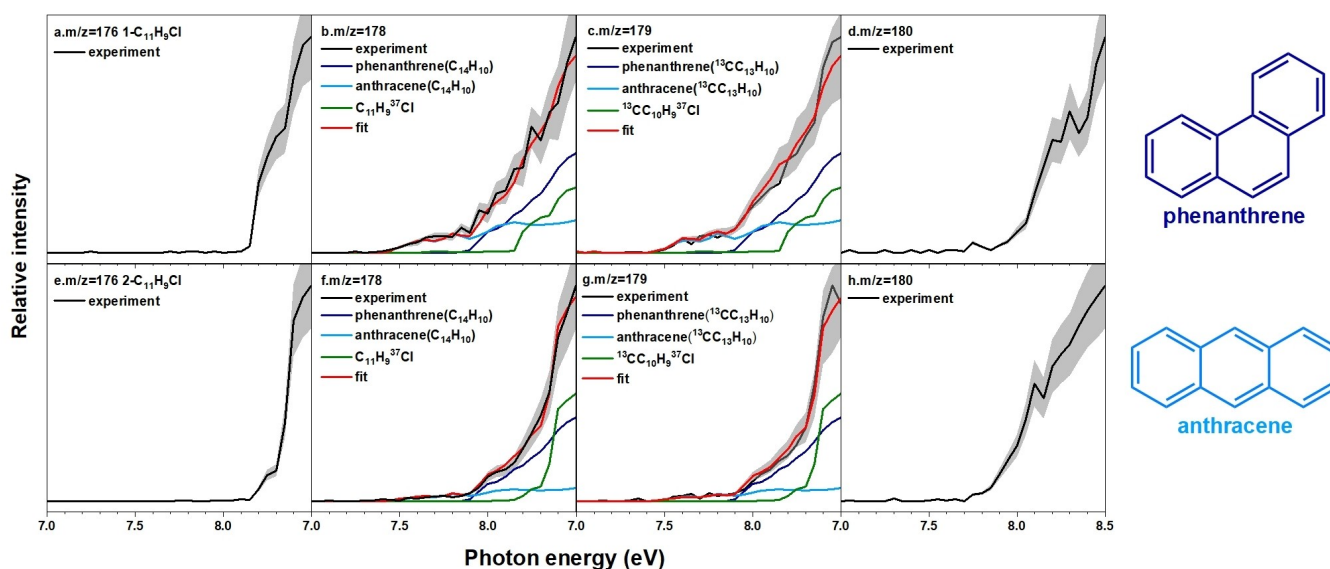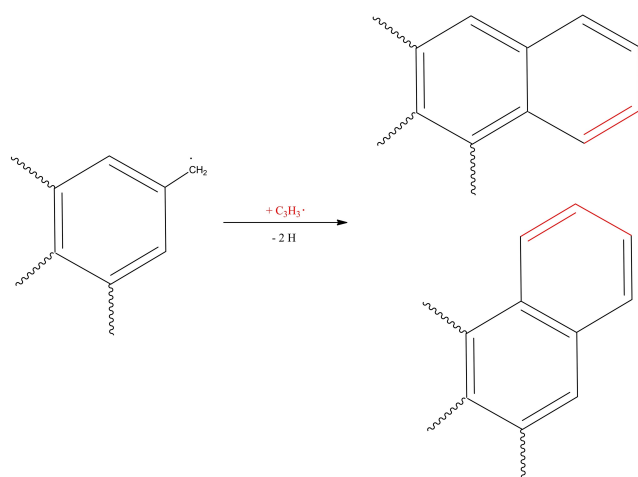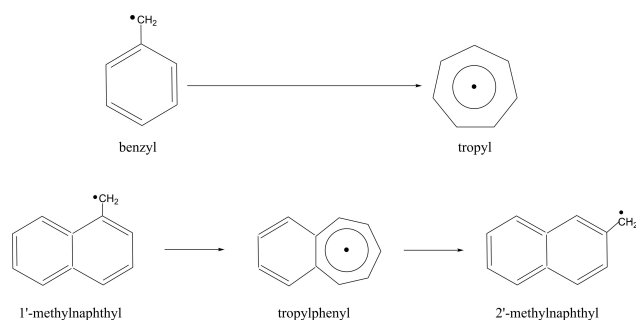

Figure 2. Experimental and reference PIE curves for species at m/z = 176, 178, 179 and 180. (a–d) 1'-chloromethylnaphthalene ($C_{11}H_9Cl$)/propargyl bromide (C_3H_3Br) system at 1,085 ± 15 K; (e–h) 2'-chloromethylnaphthalene ($C_{11}H_9Cl$)/propargyl bromide (C_3H_3Br) system at 1,085 ± 15 K. The black line refers to the normalized experimental data. The colored lines refer to the reference PIE curves of $C_{14}H_{10}$ isomers and ^{37}Cl-chloromethylnaphthalenes. The red line shows the overall fit via the linear combination of the reference curves. The overall error bars consist of two parts: ± 15% based on the accuracy of the photodiode and a 1σ error of the PIE curve averaged over the individual scans.

Conclusions

To summarize, the facile preparation the 14π Hückel aromatic polycyclic aromatic hydrocarbons anthracene and phenanthrene ($C_{14}H_{10}$) through the via the Propargyl Addition–BenzAnnulation (PABA) mechanism in conjunction with a hydrogen-assisted isomerization in the 1′- and 2′-methylnaphthyl radicals ($C_{11}H_9{}^\bullet$) – propargyl radical ($C_3H_3{}^\bullet$) systems affords persuasive testimony of the gas-phase preparation of the simplest three-ringed PAH carrying three six-membered rings under high temperature conditions in combustion flames and in circumstellar envelopes of carbon-rich stars. Whereas the concept for the formation of anthracene and phenanthrene in the 2′-methylnaphthyl – propargyl system is straightforward and can be derived from the PABA mechanism, the detection of anthracene in the 2′-methylnaphthyl – propargyl system is surprising; due to the location of the CH_2 moiety at the C1 position of the naphthalene ring, only formation of phenanthrene is expected. However, the isomerization of 1′- into 2′-methylnaphthyl via a bicyclic intermediate, which carries annulated six and seven-membered rings can rationalize the detection of anthracene. Similarly to the benzyl radical, which can de-facto isomerize to the cyclic tropyl radical (Scheme 2),[45] 1′-methylnaphthyl is expected to isomerize via a bicyclic tropylphenyl intermediate to 1′-methylnaphthyl. This effectively leads to a migration of the CH_2 moiety from the C1 to the C2 carbon atom. The high abundance of the resonantly stabilized free propargyl radical in both combustion flames[46–49] and in deep space[36] suggests that reactions with 1′- and 2′-methyl-naphthyl radicals might represent an important sink of propargyl radicals. This reaction may represent a versatile mechanistic template to more complex PAHs through the reaction of benzyl moieties, i.e. an exocyclic CH_2 unit, embedded in more complex aromatic radicals with propargyl once a neighboring aromatic C–H moiety is available for ring closure resulting in a de-facto benzene ring annulation (Scheme 3).

Scheme 2. Involvement of tropyl-type radicals in the isomerization of the 1′- to 2′-methylnaphthyl radical.

Scheme 3. Versatility of the Propargyl Addition–BenzAnnulation (PABA) mechanism in conjunction with a hydrogen-assisted isomerization leading to benzene ring annulation. The waved lines indicate the incorporation of the benzyl moiety into a larger aromatic structure; the incorporated C3 propargyl unit is color coded in red.

Experimental Section

Experiments

The experiments were conducted at the Combustion and Flame Beamline (BL03U) of the National Synchrotron Radiation Laboratory (NSRL) exploiting a high-temperature chemical reactor.[50–51] The microreactor consists of a silicon carbide (SiC) tube with a length of 40.0 mm and an inner diameter of 1.0 mm as described previously.[50] In the 1′-naphthylmethyl ($C_{11}H_9{}^\bullet$)/propargyl ($C_3H_3{}^\bullet$) experiment, a continuous beam of helium-seeded 1′-naphthylmethyl and propargyl radicals was produced in-situ via pyrolysis of 1′-chloromethylnaphthalene ($C_{11}H_9Cl$, Aladdin, >95%) and propargyl bromide (C_3H_3Br, TCL, >97%), respectively. In detail, the solid 1′-chloromethylnaphthalene precursor was placed inside a stainless-steel filter (Swagelok, SS-6F-MM-05) heated to 313 K as monitored by a type-K thermocouple. The liquid propargyl bromide was loaded in a bubbler cooled to 243 K. The helium carrier gas (> 99.999%) passed the bubbler and the filter with flow rates of 10.0 mL min^{-1} and 4.0 mL min^{-1} (STP), respectively, controlled by the MKS mass flow controllers prior to merging through a stainless steel tube at a pressure of 240 Torr; this gas mixture passed the 0.1 mm nozzle and entered the heated SiC reactor resistively heated over 20.0 mm to $1,085 \pm 15$ K measured by the type-S thermocouple. The continuous molecular beam was expanded supersonically, passed a 2.0 mm diameter skimmer located 10.0 mm downstream SiC tube, and entered the detection chamber; the latter housed a high-resolution reflection time-of-flight mass spectrometer (ReTOF-MS). The products within the supersonic molecular beam were photoionized by quasi-continuous, tunable synchrotron vacuum ultraviolet (VUV) light, extracted through an ion lens into the ReTOF-MS, and eventually detected by a microchannel plate (MCP). The photoionization efficiency (PIE) curves, which depict the ion counts as a function of photon energy at a well-defined mass-to-charge ratio (m/z), were extracted from the mass spectra recorded from 7.00 to 8.50 eV in steps of 0.05 eV. In the 2′-naphthylmethyl ($C_{11}H_9{}^\bullet$)/propargyl ($C_3H_3{}^\bullet$) system, the reaction was conducted in an analogous pattern as for the 1′-naphthylmethyl ($C_{11}H_9{}^\bullet$)/propargyl ($C_3H_3{}^\bullet$) system, but 1′-chlorome-thylnaphthalene ($C_{11}H_9Cl$, Aladdin, >95%) was replaced by 2′-chloromethylnaphthalene ($C_{11}H_9Cl$, Aladdin, >95%); the overall pressure was 200 Torr, while the SiC reactor was maintained at $1,085 \pm 15$ K.

ChemPhysChem

Research Article
doi.org/10.1002/cphc.202400151

Chemistry
Europe
European Chemical
Societies Publishing

Conflict of Interests

The authors declare no conflict of interest.

Data Availability Statement

The data that support the findings of this study are available from the corresponding author upon reasonable request.

[1] S. S. Zeichner, J. C. Aponte, S. Bhattacharjee, G. Dong, A. E. Hofmann, J. P. Dworkin, D. P. Glavin, J. E. Elsila, H. V. Graham, H. Naraoka, *Science* **2023**, *382*, 1411–1416.
[2] N. Olten, S. Senkan, *Combust. Flame* **1999**, *118*, 500–507.
[3] N. M. Marinov, W. J. Pitz, C. K. Westbrook, A. M. Vincitore, M. J. Castaldi, S. M. Senkan, C. F. Melius, *Combust. Flame* **1998**, *114*, 192–213.
[4] Y. Li, Z. Tian, L. Zhang, T. Yuan, K. Zhang, B. Yang, F. Qi, *Proc. Combust. Inst.* **2009**, *32*, 647–655.
[5] H. Richter, W. J. Grieco, J. B. Howard, *Combust. Flame* **1999**, *119*, 1–22.
[6] S. Senkan, M. Castaldi, *Combust. Flame* **1996**, *107*, 141–150.
[7] G. D. G. Peña, V. Pillai, A. Raj, J. L. Brito, *Combust. Flame* **2018**, *198*, 412–427.
[8] J. P. Longwell, in *Symposium (International) on Combustion, Vol. 19*, Elsevier, **1982**, pp. 1339–1350.
[9] Y. Li, L. Zhang, T. Yuan, K. Zhang, J. Yang, B. Yang, F. Qi, C. K. Law, *Combust. Flame* **2010**, *157*, 143–154.
[10] C. Hu, W. Li, Q. Lin, X. Cheng, Q. Huang, H. Zhang, Z. Wang, *J. Energy Inst.* **2017**, *90*, 893–901.
[11] T. Mitra, C. Chu, A. Naseri, M. J. Thomson, *Combust. Flame* **2021**, *223*, 495–510.
[12] M. H. Topal, J. Wang, Y. A. Levendis, J. B. Carlson, J. Jordan, *Fuel* **2004**, *83*, 2357–2368.
[13] M. Frenklach, E. D. Feigelson, *Astrophys. J.* **1989**, *341*, 372–384.
[14] D. S. Parker, R. I. Kaiser, T. P. Troy, M. Ahmed, *Angew. Chem. Int. Ed.* **2014**, *53*, 7740–7744.
[15] D. S. Parker, R. I. Kaiser, B. Bandyopadhyay, O. Kostko, T. P. Troy, M. Ahmed, *Angew. Chem. Int. Ed.* **2015**, *54*, 5421–5424.
[16] T. Yang, T. P. Troy, B. Xu, O. Kostko, M. Ahmed, A. M. Mebel, R. I. Kaiser, *Angew. Chem. Int. Ed.* **2016**, *55*, 14983–14987.
[17] T. Yang, R. I. Kaiser, T. P. Troy, B. Xu, O. Kostko, M. Ahmed, A. M. Mebel, M. V. Zagidullin, V. N. Azyazov, *Angew. Chem.* **2017**, *129*, 4586–4590.
[18] L. Zhao, R. I. Kaiser, B. Xu, U. Ablikim, M. Ahmed, D. Joshi, G. Veber, F. R. Fischer, A. M. Mebel, *Nat. Astron.* **2018**, *2*, 413–419.
[19] L. Zhao, S. Doddipatla, R. I. Kaiser, W. Lu, O. Kostko, M. Ahmed, L. B. Tuli, A. N. Morozov, A. H. Howlader, S. F. Wnuk, *Phys. Chem. Chem. Phys.* **2021**, *23*, 5740–5749.
[20] L. Zhao, M. B. Prendergast, R. I. Kaiser, B. Xu, U. Ablikim, M. Ahmed, B. J. Sun, Y. L. Chen, A. H. Chang, R. K. Mohamed, *Angew. Chem.* **2019**, *131*, 17603–17611.
[21] C. He, R. I. Kaiser, W. Lu, M. Ahmed, V. S. Krasnoukhov, P. S. Pivovarov, M. V. Zagidullin, V. N. Azyazov, A. N. Morozov, A. M. Mebel, *Chem. Sci.* **2023**, *14*, 5369–5378.
[22] D. S. Parker, F. Zhang, Y. S. Kim, R. I. Kaiser, A. Landera, V. V. Kislov, A. M. Mebel, A. Tielens, *Proc. Natl. Acad. Sci. USA* **2012**, *109*, 53–58.
[23] L. Zhao, R. I. Kaiser, B. Xu, U. Ablikim, M. Ahmed, M. V. Zagidullin, V. N. Azyazov, A. H. Howlader, S. F. Wnuk, A. M. Mebel, *J. Phys. Chem. Lett.* **2018**, *9*, 2620–2626.
[24] L. Zhao, R. I. Kaiser, B. Xu, U. Ablikim, M. Ahmed, M. M. Evseev, E. K. Bashkirov, V. N. Azyazov, A. M. Mebel, *Nat. Astron.* **2018**, *2*, 973–979.
[25] L. Zhao, B. Xu, U. Ablikim, W. Lu, M. Ahmed, M. M. Evseev, E. K. Bashkirov, V. N. Azyazov, A. H. Howlader, S. F. Wnuk, *ChemPhysChem* **2019**, *20*, 791–797.
[26] L. Zhao, R. I. Kaiser, B. Xu, U. Ablikim, M. Ahmed, M. M. Evseev, E. K. Bashkirov, V. N. Azyazov, M. V. Zagidullin, *Nat. Commun.* **2019**, *10*, 1510.
[27] R. I. Kaiser, L. Zhao, W. Lu, M. Ahmed, M. M. Evseev, V. N. Azyazov, A. M. Mebel, R. K. Mohamed, F. R. Fischer, X. Li, *Phys. Chem. Chem. Phys.* **2022**, *24*, 25077–25087.
[28] L. Zhao, R. I. Kaiser, B. Xu, U. Ablikim, M. Ahmed, M. M. Evseev, E. K. Bashkirov, V. N. Azyazov, A. M. Mebel, *Angew. Chem.* **2020**, *132*, 4080–4087.
[29] L. Zhao, R. I. Kaiser, W. Lu, M. Ahmed, M. M. Evseev, E. K. Bashkirov, V. N. Azyazov, C. Tönshoff, F. Reicherter, H. F. Bettinger, *Angew. Chem. Int. Ed.* **2020**, *59*, 11334–11338.
[30] S. Doddipatla, G. R. Galimova, H. Wei, A. M. Thomas, C. He, Z. Yang, A. N. Morozov, C. N. Shingledecker, A. M. Mebel, R. I. Kaiser, *Sci. Adv.* **2021**, *7*, eabd4044.
[31] W. Li, J. Yang, L. Zhao, D. Couch, M. San Marchi, N. Hansen, A. N. Morozov, A. M. Mebel, R. I. Kaiser, *Chem. Sci.* **2023**, *14*, 9795–9805.
[32] I. Cherchneff, J. R. Barker, A. G. Tielens, *Astrophys. J.* **1992**, *401*, 269–287.
[33] M. Cohen, A. Tielens, J. Bregman, *Astrophys. J.* **1989**, *344*, L13–L16.
[34] E. Micelotta, A. Jones, A. Tielens, *Astron. Astrophys.* **2010**, *510*, A36.
[35] D. Williams, in *Symposium-International Astronomical Union, Vol. 197*, Cambridge University Press, **2000**, pp. 549–554.
[36] M. Agúndez, C. Cabezas, B. Tercero, N. Marcelino, J. Gallego, P. de Vicente, J. Cernicharo, *Astron. Astrophys.* **2021**, *647*, L10.
[37] D. S. Parker, B. B. Dangi, R. I. Kaiser, A. Jamal, M. N. Ryazantsev, K. Morokuma, A. Korte, W. Sander, *J. Phys. Chem. A* **2014**, *118*, 2709–2718.
[38] T. Yang, L. Muzangwa, R. I. Kaiser, A. Jamal, K. Morokuma, *Phys. Chem. Chem. Phys.* **2015**, *17*, 21564–21575.
[39] M. Zagidullin, R. Kaiser, D. Porfiriev, I. Zavershinskiy, M. Ahmed, V. Azyazov, A. Mebel, *J. Phys. Chem. A* **2018**, *122*, 8819–8827.
[40] T. Yang, R. I. Kaiser, T. P. Troy, B. Xu, O. Kostko, M. Ahmed, A. M. Mebel, M. V. Zagidullin, V. N. Azyazov, *Angew. Chem. Int. Ed.* **2017**, *56*, 4515–4519.
[41] C. He, R. I. Kaiser, W. Lu, M. Ahmed, Y. Reyes, S. F. Wnuk, A. M. Mebel, *J. Am. Chem. Soc.* **2023**, *145*, 3084–3091.
[42] J. W. Hager, S. C. Wallace, *Anal. Chem.* **1988**, *60*, 5–10.
[43] N. Thantu, P. M. Weber, *Chem. Phys. Lett.* **1993**, *214*, 276–280.
[44] Y. Y. Li, J; Cheng, Z., Photoionization Cross Section Database (Version 2.0). National Synchrotron Radiation Laboratory, Hefei, China, 2017.
[45] G. T. Buckingham, J. P. Porterfield, O. Kostko, T. P. Troy, M. Ahmed, D. J. Robichaud, M. R. Nimlos, J. W. Daily, G. B. Ellison, *J. Chem. Phys.* **2016**, *145*, 014305.
[46] H.-A. Gueniche, P.-A. Glaude, G. Dayma, R. Fournet, F. Battin-Leclerc, *Combust. Flame* **2006**, *146*, 620–634.
[47] N. M. Marinov, M. J. Castaldi, C. F. Melius, W. Tsang, *Combust. Sci. Technol.* **1997**, *128*, 295–342.
[48] M. Kamphus, M. Braun-Unkhoff, K. Kohse-Höinghaus, *Combust. Flame* **2008**, *152*, 28–59.
[49] C. S. McEnally, L. D. Pfefferle, B. Atakan, K. Kohse-Höinghaus, *Prog. Energy Combust. Sci.* **2006**, *32*, 247–294.
[50] W. Li, L. Zhao, R. I. Kaiser, *Phys. Chem. Chem. Phys.* **2023**, *25*, 4141–4150.
[51] Z. Zhou, X. Du, J. Yang, Y. Wang, C. Li, S. Wei, L. Du, Y. Li, F. Qi, Q. Wang, *J. Synchrotron Radiat.* **2016**, *23*, 1035–1045.